

NON-FERMI-LIQUID BEHAVIOR IN THE FLUCTUATING GAP MODEL: FROM THE POLE TO A ZERO OF THE GREEN'S FUNCTION

*E. Z. Kuchinskii, M. V. Sadovskii**

*Institute for Electrophysics, Russian Academy of Sciences
620016, Ekaterinburg, Russia*

Received February 17, 2006

We analyze the non-Fermi-liquid (NFL) behavior of the fluctuating gap model (FGM) of pseudogap behavior in both one and two dimensions. A detailed discussion of the quasiparticle renormalization (Z -factor) is given, demonstrating a kind of “marginal” Fermi-liquid or Luttinger-liquid behavior and topological stability of the “bare” Fermi surface (the Luttinger theorem). In the two-dimensional case, we discuss the effective picture of the Fermi surface “destruction” both in “hot spot” model of dielectric (AFM, CDW) pseudogap fluctuations and for the qualitatively different case of superconducting d -wave fluctuations, reflecting the NFL spectral density behavior and similar to that observed in ARPES experiments on copper oxides.

PACS: 71.10.Hf, 71.27.+a, 74.72.-h

1. INTRODUCTION

Pseudogap formation in the electronic spectrum of underdoped copper oxides is an especially striking anomaly of the normal state of high-temperature superconductors [1]. Discussions on the nature of the pseudogap state continue within two main “scenarios” — of superconducting fluctuations, leading to Cooper pair formation above T_c , or of other order-parameter fluctuations, in fact competing with superconductivity.

We believe that the preferable scenario for pseudogap formation is most likely based on the model of strong scattering of the charge carriers by short-range antiferromagnetic (AFM, SDW) spin fluctuations [1]. In momentum representation, this scattering transfers momenta of the order of $\mathbf{Q} = (\pi/a, \pi/a)$ (where a is the lattice constant of a two-dimensional lattice). This leads to the formation of structures in the one-particle spectrum that are precursors of the changes in the spectra due to a long-range AFM order (period doubling).

Within this spin-fluctuation scenario, a simplified model of the pseudogap state was studied [1–3] under the assumption that the scattering by dynamic spin fluctuations can be reduced for high enough temperatures to a static Gaussian random field (quenched disorder)

of pseudogap fluctuations. These fluctuations are defined by a characteristic scattering vector from the vicinity of \mathbf{Q} , with a width determined by the inverse correlation length of the short-range order $\kappa = \xi^{-1}$. Actually, a similar model (formalism) can also be applied to the case of pseudogaps of a superconducting nature [3].

These models originated from the earlier one-dimensional model of pseudogap behavior [4, 5], the so-called fluctuating gap model (FGM), which is exactly solvable in the asymptotic limit of large correlation lengths of pseudogap fluctuations $\kappa = \xi^{-1} \rightarrow 0$ [4], and “nearly exactly” solvable in the case of finite κ , where we can take all Feynman diagrams of perturbation series into account, albeit using an approximate ansatz for higher-order contributions [5].

Non-Fermi-liquid behavior of the FGM model was already discussed in one [4, 6–8] and two dimensions [1–3]. However, some interesting aspects of this model are still under discussion [9]. Below, we analyze different aspects of this anomalous behavior in both one- and two-dimensional versions, mainly in the case of AFM (SDW) or CDW pseudogap fluctuations, and also, more briefly, in the case of superconducting fluctuations, demonstrating a kind of “marginal” Fermi-liquid behavior and the qualitative picture of Fermi surface

*E-mail: sadovskii@iep.uran.ru

“destruction” and formation of “Fermi arcs” in two dimensions, similar to those observed in ARPES experiments on copper oxides.

2. POSSIBLE TYPES OF GREEN'S FUNCTION RENORMALIZATION

We start with a qualitative discussion of possible manifestations of the NFL behavior. The Green's function of the interacting system of electrons is expressed via the Dyson equation (in the Matsubara representation, with $\varepsilon_n = (2n + 1)\pi T$ and $\xi_p = v_F(p - p_F)$) as¹⁾

$$G(\varepsilon_n, \xi_p) = \frac{1}{i\varepsilon_n - \xi_p - \Sigma(\varepsilon_n, \xi_p)}. \quad (1)$$

In what follows, we use a rather unusual definition of the renormalization (“residue”) Z -factor, introducing it as [9]

$$G(\varepsilon_n, \xi_p) = Z(\varepsilon_n, \xi_p)G_0(\varepsilon_n, \xi_p) = \frac{Z(\varepsilon_n, \xi_p)}{i\varepsilon_n - \xi_p} \quad (2)$$

or

$$Z(\varepsilon_n, \xi_p) = \frac{i\varepsilon_n - \xi_p}{i\varepsilon_n - \xi_p - \Sigma(\varepsilon_n, \xi_p)} = (i\varepsilon_n - \xi_p)G(\varepsilon_n, \xi_p). \quad (3)$$

We note that $Z(\varepsilon_n, \xi_p)$ is in general complex and actually determines the full renormalization of the free-electron Green's function $G_0(\varepsilon_n, \xi_p)$ due to interactions. At the same time, it is in some sense similar to the standard residue renormalization factor used in the Fermi-liquid theory.

We consider possible alternatives for the $Z(\varepsilon_n, \xi_p)$ behavior.

A. Fermi-liquid behavior

In a normal Fermi liquid, we can perform the usual expansion (close to the Fermi level and in the obvious notation) assuming the absence of any singularities in $\Sigma(\varepsilon_n, p)$:

$$\Sigma(\varepsilon_n, \xi_p) \approx \Sigma(0, 0) + i\varepsilon_n \left. \frac{\partial \Sigma(\varepsilon_n, \xi_p)}{\partial (i\varepsilon_n)} \right|_0 + \xi_p \left. \frac{\partial \Sigma(\varepsilon_n, \xi_p)}{\partial \xi_p} \right|_0 + \dots \quad (4)$$

¹⁾ Despite our use of the Matsubara representation, we regard ε_n as a continuous variable below.

In the absence of the static impurity scattering, $\Sigma(0, 0)$ is real and just renormalizes the chemical potential. We can then rewrite (1) as

$$G(\varepsilon) = \frac{1}{i\varepsilon_n \left\{ 1 - \frac{\partial \Sigma}{\partial (i\varepsilon_n)} \right\}_0 - \xi_p \left\{ 1 + \frac{\partial \Sigma}{\partial \xi_p} \right\}_0} \equiv \frac{\tilde{Z}}{i\varepsilon_n - \tilde{\xi}_p}, \quad (5)$$

where we have introduced the usual renormalized residue at the pole,

$$\tilde{Z} = \frac{1}{1 - \left. \frac{\partial \Sigma}{\partial (i\varepsilon_n)} \right|_0}, \quad \tilde{Z}^{-1} = 1 - \left. \frac{\partial \Sigma}{\partial (i\varepsilon_n)} \right|_0, \quad (6)$$

and the spectrum of quasiparticles

$$\tilde{\xi}_p = \tilde{Z} \left(1 + \frac{\partial \Sigma}{\partial \xi_p} \right)_0 \xi_p. \quad (7)$$

The usual analytic continuation to real frequencies now yields the standard expressions of the normal Fermi-liquid theory [10, 11] with real $0 < \tilde{Z} < 1$, conserving the quasiparticle pole of the Green's function.

In the special case where $\xi_p = 0$, i.e., at the Fermi surface, which is not renormalized by interactions in accordance with the Landau hypothesis and Luttinger theorem, we have

$$G(\varepsilon_n, \xi_p) = \frac{\tilde{Z}}{i\varepsilon_n}, \quad (8)$$

i.e., \tilde{Z} coincides with the limit of $Z(\varepsilon_n \rightarrow 0, \xi_p = 0)$ defined by (2) and (3), and we have the usual pole as $\varepsilon_n \rightarrow 0$. Similarly, for $\varepsilon_n = 0$, we have $Z(\varepsilon_n = 0, \xi_p \rightarrow 0) \sim \tilde{Z}$.

In general, this behavior is preserved not only in the case of $\Sigma(\varepsilon_n, \xi_p)$ possessing a regular expansion at small ε_n and ξ_p , but also for $\Sigma(\varepsilon_n, \xi_p) \sim \max(\varepsilon_n^\alpha, \xi_p^\alpha)$ with any $\alpha \geq 1$.

B. Impure Fermi liquid

In the case of low concentration of random static impurities, we have $\Sigma(\varepsilon_n \rightarrow 0, \xi_p \rightarrow 0) \rightarrow \text{const}$, with $\text{Re } \Sigma(0, 0)$ again giving a shift of the chemical potential, while $\text{Im } \Sigma(0, 0) \sim \gamma$, where γ is the impurity scattering rate. For the Green's function, we have

$$G(\varepsilon_n, \xi_p) = \frac{\tilde{Z}}{i\varepsilon_n - \tilde{\xi}_p + i\gamma \frac{\varepsilon_n}{|\varepsilon_n|}} \quad (9)$$

and hence the renormalization factor defined by (3) is given by

$$Z(\varepsilon_n, \xi_p) = \tilde{Z} \frac{i\varepsilon_n - \xi_p}{i\varepsilon_n - \tilde{\xi}_p + i\gamma \frac{\varepsilon_n}{|\varepsilon_n|}}. \quad (10)$$

For $\xi_p = 0$, we have

$$\begin{aligned} Z(\varepsilon_n, \xi_p = 0) &= \tilde{Z} \frac{i\varepsilon_n}{i\varepsilon_n + i\gamma \frac{\varepsilon_n}{|\varepsilon_n|}} \sim \\ &\sim \frac{|\varepsilon_n|}{\gamma} \rightarrow 0 \quad \text{as } |\varepsilon_n| \rightarrow 0 \end{aligned} \quad (11)$$

and for $|\varepsilon_n| \ll |\xi_p|$,

$$\begin{aligned} Z(\varepsilon_n \rightarrow 0, \xi_p) &= \tilde{Z} \frac{\xi_p}{\xi_p - i\gamma \frac{\varepsilon_n}{|\varepsilon_n|}} \sim \\ &\sim \frac{\xi_p}{\gamma} \text{sign } \varepsilon_n \rightarrow 0 \quad \text{as } \xi_p \rightarrow 0, \end{aligned} \quad (12)$$

i.e., impurity scattering leads to the vanishing of the Z -factor at the Fermi surface, just removing the usual Fermi-liquid pole singularity and producing a finite discontinuity of the Green's function at $\varepsilon_n = 0$. This behavior is due to the loss of translational invariance of the Fermi liquid theory (momentum conservation) because of impurities. In fact, Green's function (9) is obtained after averaging over the impurity position, which formally restores translational invariance, leading to a kind of (trivial) non-Fermi-liquid (NFL) behavior. We note that this behavior is observed for $|\varepsilon_n|, |\xi_p| \ll \gamma$, while in the opposite limit, we obviously have a finite $Z(\varepsilon, \xi_p) \sim \tilde{Z}$.

C. Superconductors and Peierls and excitonic insulators

We now consider the case of an s -wave superconductor. The normal Gorkov Green's function is given by

$$G(\varepsilon_n, \xi_p) = \frac{i\varepsilon_n + \xi_p}{(i\varepsilon_n)^2 - \xi_p^2 - |\Delta|^2}, \quad (13)$$

where Δ is the superconducting gap. The normal Green's function also takes this form in an excitonic or Peierls insulator, where Δ denotes the appropriate insulating gap in the spectrum [11]. Then

$$\begin{aligned} Z(\varepsilon_n, \xi_p) &= \frac{(i\varepsilon_n)^2 - (\xi_p)^2}{(i\varepsilon_n)^2 - \xi_p^2 - |\Delta|^2} \sim \\ &\sim \frac{\max(\varepsilon_n^2, \xi_p^2)}{|\Delta|^2} \rightarrow 0 \quad \text{for } \varepsilon_n, \xi_p \rightarrow 0, \end{aligned} \quad (14)$$

i.e., we have the NFL behavior with the pole of the Green's function at the Fermi surface replaced by a zero, due to the Fermi surface being "closed" by the superconducting (or insulating) gap.

Again, Fermi-liquid-type behavior with a finite Z -factor is "restored" for $|\varepsilon_n|, |\xi_p| \gg |\Delta|$.

But the complete description of the superconducting (excitonic, Peierls) phase is achieved only after the introduction of the anomalous Gorkov function. The excitation spectrum on both sides of the phase transition is determined by different Green's functions with different topological properties [9].

D. Non-Fermi-liquid behavior due to interactions

Non-Fermi-liquid behavior of Green's function due to interactions may also occur in the case of the singular behavior $\Sigma(\varepsilon_n, \xi_p) \rightarrow \infty$ as $\varepsilon_n \rightarrow 0$ and $\xi_p \rightarrow 0$, e.g., a power-like divergence²⁾ of $\Sigma(\varepsilon_n, \xi_p) \sim \max(\varepsilon_n^{-\alpha}, \xi_p^{-\alpha})$ with $\alpha > 0$. Obviously, $Z(\varepsilon_n \rightarrow 0, \xi_p \rightarrow 0) \rightarrow 0$ in this case, and we again have a zero of the Green's function at the Fermi surface.

Another possibility is a singular behavior of derivatives of the self-energy in (4), e.g., in the case where $\Sigma(\varepsilon_n, \xi_p) \sim \max(\varepsilon_n^\alpha, \xi_p^\alpha)$ with $0 < \alpha < 1$, leading to the pole singularity of the Green's function at the Fermi surface being weaker than usual.

Both types of behavior are realized within the Tomonaga–Luttinger model in one dimension [12], where the asymptotic behavior of $G(i\varepsilon_n, \xi_p)$ in the region of small $\xi_p \sim \varepsilon_n$ can be expressed as

$$G(\varepsilon_n \sim \xi_p) \sim \frac{1}{\varepsilon_n^{1-2\alpha'}} \quad (15)$$

with $\alpha' < 1/2$. For $\alpha' > 1/2$,

$$G(\varepsilon_n \sim \xi_p) \sim A + B\varepsilon_n^{2\alpha'-1}. \quad (16)$$

For $3/2 > \alpha' > 1$,

$$G(\varepsilon_n \sim \xi_p) \sim A + B\varepsilon_n + C\varepsilon_n^{2\alpha'-1}, \quad (17)$$

etc., with the value of α' determined by the interaction strength.

A special case is given by the so-called "marginal" Fermi-liquid behavior assumed [13] for the interpretation of the electronic properties of CuO₂ planes of copper oxides. It is given by

$$\Sigma(\varepsilon_n, \xi_p) \sim \lambda i\varepsilon_n \ln \frac{\max(\varepsilon_n, \xi_p)}{\omega_c}, \quad (18)$$

²⁾ An additional logarithmic divergence can also be present here!

where λ is some dimensionless interaction constant and ω_c is a characteristic cut-off frequency. If we formally use (6) at finite ε_n , we obtain

$$\tilde{Z}(\varepsilon_n, \xi_p) \sim \frac{1}{1 - \lambda \ln \frac{\max(\varepsilon_n, \xi_p)}{\omega_c}}. \quad (19)$$

In this case, the “residue at the pole” of the Green’s function (Z -factor)³⁾ tends to zero at the Fermi surface itself, and, again, quasiparticles are just not defined there at all! However, everywhere outside a narrow (logarithmic) region close to the Fermi surface, we have a more or less “usual” quasiparticle contribution: quasiparticles (close to the Fermi surface) are just “marginally” defined. At present, there are no generally accepted microscopic models of the “marginal” Fermi-liquid behavior in two dimensions.

3. FLUCTUATING GAP MODEL

The physical nature of the FGM was extensively discussed in the literature [1–8, 11]. The model based on the picture of an electron propagating in the (static!) Gaussian random field of (pseudogap) fluctuations, leading to scattering with the characteristic momentum transfer from a close vicinity of some fixed scattering vector \mathbf{Q} . These fluctuations are described by two basic parameters: the amplitude Δ and the correlation length (of short-range order) ξ^{-1} , determining the effective width $\kappa = \xi^{-1}$ of the scattering vector distribution.

In one dimension, the typical choice of the scattering vector is $Q = 2p_F$ (the fluctuation region of the Peierls transition) [4, 5], while in two dimensions, we usually mean the so-called “hot spot” model with $\mathbf{Q} = (\pi/a, \pi/a)$ [2, 3]. These models assume the “dielectric” (CDW, SDW) nature of pseudogap fluctuations, but essentially the same formalism can be used in the case of superconducting fluctuations [3].

The case of superconducting (s -wave) pseudogap fluctuations in higher dimensions is actually described by the same one-dimensional version of the FGM [3, 4, 9].

An attractive property of the models under discussion is the possibility of an exact solution achieved by the complete summation of the whole Feynman diagram series in the asymptotic limit of large correlation

lengths $\xi \rightarrow \infty$ [4, 6]. In the case of finite correlation lengths, we can also perform summation of all Feynman diagrams for the single-electron Green’s function using an approximate ansatz for higher-order contributions in both one [5] and two dimensions [2, 3]. Similar methods of diagram summation can also be applied in calculations of the two-particle Green’s functions (vertex parts) [2–4, 7, 11, 14].

Our aim is to demonstrate that nearly all aspects of the NFL behavior discussed above can be nicely described within different variants of the FGM.

A. One dimension

We limit ourselves here to the case of incommensurate pseudogap (CDW) fluctuations [4, 5]. The commensurate case [6, 5] can be analyzed similarly. We note that the same expressions also apply in the case of superconducting (s -wave) fluctuations in all dimensions.

In the limit of the infinite correlation length of pseudogap fluctuations, we have the exact solution for a single-electron Green’s function [4, 11] given by

$$\begin{aligned} G(\varepsilon_n, \xi_p) &= \int_0^\infty d\zeta e^{-\zeta} \frac{i\varepsilon_n + \xi_p}{(i\varepsilon_n)^2 - \xi_p^2 - \zeta\Delta^2} = \\ &= \frac{i\varepsilon_n + \xi_p}{\Delta^2} \exp\left(\frac{\varepsilon_n^2 + \xi_p^2}{\Delta^2}\right) \text{Ei}\left(\frac{\varepsilon_n^2 + \xi_p^2}{\Delta^2}\right) \approx \\ &\approx \frac{i\varepsilon_n + \xi_p}{\Delta^2} \ln\left(\gamma' \frac{\varepsilon_n^2 + \xi_p^2}{\Delta^2}\right) \\ &\text{as } \varepsilon_n \rightarrow 0, \quad \xi_p \rightarrow 0, \quad (20) \end{aligned}$$

where $\text{Ei}(-x)$ denotes the integral exponential function and we use the asymptotic behavior $\text{Ei}(-x) \sim \ln(\gamma'x)$ as $x \rightarrow 0$ ($\ln \gamma' = 0.577$ is the Euler constant). Then, using (3), we immediately obtain

$$\begin{aligned} Z(\varepsilon_n, \xi_p) &= -\frac{\varepsilon_n^2 + \xi_p^2}{\Delta^2} \ln\left(\gamma' \frac{\varepsilon_n^2 + \xi_p^2}{\Delta^2}\right) \rightarrow 0 \\ &\text{as } \varepsilon_n \rightarrow 0, \quad \xi_p \rightarrow 0. \quad (21) \end{aligned}$$

Precisely the same result is obtained if, for finite ε_n and ξ_p , we define

$$\tilde{Z}(\varepsilon_n, \xi_p) = \frac{1}{1 - \frac{\partial \Sigma(\varepsilon_n, \xi_p)}{\partial (i\varepsilon_n)}} \quad (22)$$

³⁾ We note that (19), strictly speaking, cannot give the correct definition of the “residue”, because standard expression (6) is defined only at the Fermi surface itself, where (19) just does not exist. In what follows, we therefore prefer the rather unusual definition in (2).

similarly to (6). We note that because $|\varepsilon_n| \ll \Delta$ and $|\xi_p| \ll \Delta$, we obviously have $Z > 0$, but the usual pole of the Green's function at the Fermi surface ("point") of the "normal" system is here transformed into a zero due to pseudogap fluctuations. Because of the topological stability [9], the singularity of the Green's function at the Fermi surface is not destroyed: the zero is also a singularity (with the same topological charge) as the pole. But the FGM actually gives an explicit example of a kind of Luttinger or "marginal" Fermi liquid with a very strong renormalization of the singularity at the Fermi surface.

We consider the self-energy corresponding to Green's functions (20):

$$\Sigma(\varepsilon_n, \xi_p) = i\varepsilon_n - \xi_p - \left[\int_0^\infty d\zeta e^{-\zeta} \frac{i\varepsilon_n + \xi_p}{(i\varepsilon_n)^2 - \xi_p^2 - \zeta\Delta^2} \right]^{-1}. \quad (23)$$

$$Z(\varepsilon_n, \xi_p) = \frac{i\varepsilon_n - \xi_p}{i\varepsilon_n - \xi_p - \frac{\Delta^2}{i\varepsilon_n + \xi_p + iv_F\kappa - \frac{\Delta^2}{i\varepsilon_n - \xi_p + 2iv_F\kappa - \frac{2\Delta^2}{i\varepsilon_n + \xi_p + 3iv_F\kappa - \dots}}}}, \quad (25)$$

which can be studied numerically.

In Fig. 1, we show typical dependences of the renormalization factor $Z(\varepsilon_n, \xi_p)$. In all cases, it tends to zero at the ("bare") Fermi surface and the pole of the Green's function disappears. Essentially, this strong renormalization starts on the scale of the pseudogap width, i.e., for $|\varepsilon_n| < \Delta$ and $|\xi_p| < \Delta$, reflecting a non-Fermi-liquid behavior due to pseudogap fluctuations.

However, the role of finite correlation lengths ξ (finite κ) is qualitatively similar to static impurity scattering⁴⁾, and a more detailed calculation shows that the Z-factor behaves at small $\varepsilon_n \ll v_F\kappa$ and $|\xi_p| \ll v_F\kappa$ (with $\varepsilon_n > 0$) as

$$Z(\varepsilon_n, \xi_p) \approx \alpha \left(\frac{v_F\kappa}{\Delta} \right) \left(\frac{\varepsilon_n + i\xi_p}{\Delta} \right) \rightarrow 0 \quad \text{as } \varepsilon_n \rightarrow 0, \quad \xi_p \rightarrow 0, \quad (26)$$

with $\alpha(v_F\kappa/\Delta) \rightarrow 0$ as $\kappa \rightarrow 0$, as seen from Fig. 2. In terms of the Green's function, this behavior corresponds to

⁴⁾ This is due to our approximation of the static nature of pseudogap fluctuations.

Taking $\xi_p = 0$ for simplicity and $\varepsilon_n \rightarrow 0$, we obtain

$$\Sigma(\varepsilon_n \rightarrow 0, \xi_p = 0) = \frac{1}{i\varepsilon_n} \left[\int_0^\infty d\zeta e^{-\zeta} \frac{1}{\varepsilon_n^2 + \zeta\Delta^2} \right]^{-1} \approx -\frac{\Delta^2}{i\varepsilon_n} \frac{1}{\ln\left(\gamma' \frac{\varepsilon_n^2}{\Delta^2}\right)} \rightarrow \infty, \quad (24)$$

i.e., the divergence of the type discussed above.

In the case of finite correlation lengths $\xi = \kappa^{-1}$ of pseudogap fluctuations, we use the continuous-fraction representation of single-electron Green's function derived in Ref. [5] to obtain the renormalization factor as ($\varepsilon_n > 0$)

$$G(\varepsilon_n, \xi_p) \approx \frac{1}{\Delta} \alpha \left(\frac{v_F\kappa}{\Delta} \right) \frac{\varepsilon_n + i\xi_p}{i\varepsilon_n - \xi_p} = -i \frac{1}{\Delta} \alpha \left(\frac{v_F\kappa}{\Delta} \right). \quad (27)$$

Therefore, for finite κ , the Green's function has no zero at $\varepsilon_n = 0$ and $\xi_p = 0$ and remains finite as in an impure system.

The vanishing of the renormalization factor $Z(\varepsilon_n, \xi_p)$ at the "bare" Fermi surface is in correspondence with the general topological stability arguments [9]: in the absence of static impurity-like scattering, the pole singularity of the Green's function is replaced by a zero. In the presence of this additional scattering, this zero is replaced by a finite discontinuity, and the singularity therefore persists.

B. "Hot spot" model in two dimensions

In two dimensions, we introduce the so-called "hot spot" model. We consider a typical Fermi surface of electrons moving in the CuO₂ plane of copper oxides as shown in Fig. 3. If we neglect fine details, the observed (e.g., in ARPES experiments) Fermi surface (and also

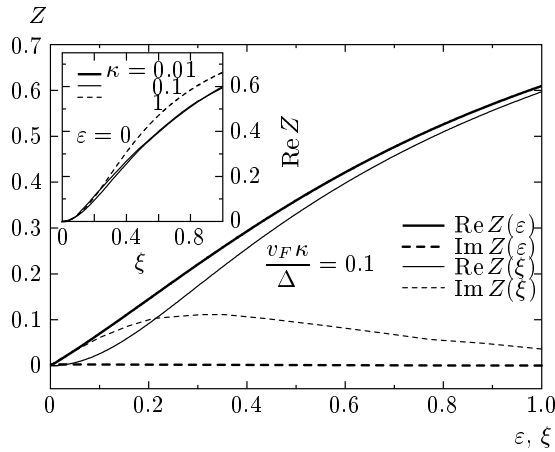


Fig. 1. Typical dependences of the $Z(\varepsilon_n, \xi_p)$ factor in the one-dimensional FGM with finite correlation lengths: dependences of $Z(\varepsilon_n = 0, \xi_p)$ and $Z(\varepsilon_n, \xi_p = 0)$ on ε_n and ξ_p for $v_F \kappa / \Delta = 0.1$. Inset: the dependences of $\text{Re} Z(\varepsilon_n = 0, \xi_p)$ on ξ_p for different values of κ (in units of Δ/v_F). Both ε_n and ξ_p are given in units of Δ

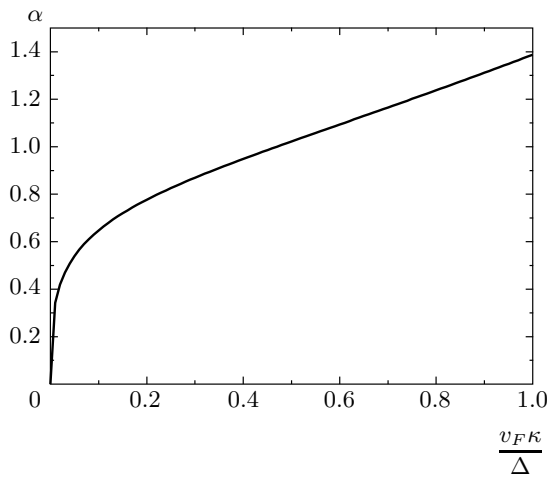


Fig. 2. Dependence of $\alpha(v_F \kappa / \Delta)$ on the inverse correlation length

the spectrum of elementary excitations) in the CuO_2 plane is in the first approximation described by the usual tight-binding model,

$$\epsilon(\mathbf{p}) = -2t(\cos p_x a + \cos p_y a) - 4t' \cos p_x a \cos p_y a, \quad (28)$$

where t is the nearest-neighbor transfer integral, t' is the transfer integral between second-nearest neighbors, and a is the square lattice constant.

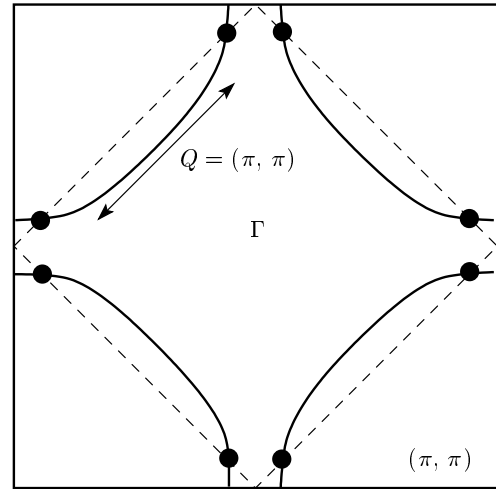


Fig. 3. Fermi surface in the Brillouin zone and the “hot spot” model. The magnetic zone appears, e.g., in the presence of the antiferromagnetic long-range order. “Hot spots” correspond to intersections of the magnetic zone borders with the Fermi surface and are connected by the scattering vector of the order of $\mathbf{Q} = (\pi/a, \pi/a)$

Phase transition to the antiferromagnetic state induces lattice period doubling and leads to the appearance of an “antiferromagnetic” Brillouin zone in inverse space, as is also shown in Fig. 3. If the spectrum of carriers is given by (28) with $t' = 0$ and we consider the half-filled case, the Fermi surface becomes just a square coinciding with the borders of the antiferromagnetic zone and we have a complete “nesting”: flat parts of the Fermi surface match each other after the translation by the vector of antiferromagnetic ordering $\mathbf{Q} = (\pm\pi/a, \pm\pi/a)$. In this case and for $T = 0$, the electron spectrum is unstable, the energy gap appears everywhere on the Fermi surface, and the system becomes an insulator, due to the formation of an antiferromagnetic spin density wave (SDW)⁵⁾. In the case of the Fermi surface shown in Fig. 3, the appearance of the antiferromagnetic long-range order, in accordance with the general rules of the band theory, leads to the appearance of discontinuities of isoenergetic surfaces (e.g., the Fermi surface) at crossing points with boundaries of a new (magnetic) Brillouin zone due to gap opening at points connected by the vector \mathbf{Q} .

In the most part of the underdoped region of the cuprate phase diagram, the antiferromagnetic long-range order is absent, but a number of experiments sup-

⁵⁾ Analogous dielectrization is also realized in the case of the formation of the similar charge density wave (CDW).

port the existence of well-developed fluctuations of the antiferromagnetic short-range order that scatter electrons with the characteristic momentum transfer of the order of \mathbf{Q} . Similar effects may appear due to CDW fluctuations. These pseudogap fluctuations are again considered to be static and Gaussian, and characterized by two parameters: the amplitude Δ and correlation length $\xi = \kappa^{-1}$ [1]. In this case, we can obtain a rather complete solution for the single-electron Green's function via summation of all Feynman diagrams of the perturbation series describing scattering by these fluctuations [1–3]. This solution is again exact in the limit as $\xi \rightarrow \infty$ [2], and apparently very close to the exact solution in case of finite ξ [15]. Generalizations of this approach to two-particle properties (vertex parts) are also quite feasible.

We start again with an exact solution for $\xi \rightarrow \infty$ (or $\kappa = 0$) [2]. We first introduce the (normal) Green's function for the SDW (CDW) state with long-range order (see, e.g., [11]):

$$G(\varepsilon_n, \xi_{\mathbf{p}}) = \frac{i\varepsilon_n - \xi_{\mathbf{p}-\mathbf{Q}}}{(i\varepsilon_n - \xi_{\mathbf{p}})(i\varepsilon_n - \xi_{\mathbf{p}-\mathbf{Q}}) - W^2}, \quad (29)$$

where W denotes the amplitude of the SDW (CDW) periodic potential and $\xi_{\mathbf{p}} = \varepsilon(\mathbf{p}) - \mu$. Then we can write the appropriate Z factor as

$$Z(\varepsilon_n, \xi_{\mathbf{p}}) = \frac{(i\varepsilon_n - \xi_1)(i\varepsilon_n - \xi_2)}{(i\varepsilon_n - \xi_1)(i\varepsilon_n - \xi_2) - W^2}, \quad (30)$$

where we set $\xi_{\mathbf{p}} = \xi_1$ and $\xi_{\mathbf{p}-\mathbf{Q}} = \xi_2$ for brevity. In what follows, we are mainly interested in the limit as $\varepsilon_n \rightarrow 0$ and $\xi_1 \rightarrow 0$, i.e., in the vicinity of the “bare” Fermi surface. We note that $\xi_2 = 0$ defines the so-called “shadow” Fermi surface. We have $\xi_1 = \xi_2 = 0$ precisely at the “hot spots”. It is convenient to introduce the complex variable

$$z = (i\varepsilon_n - \xi_1)(i\varepsilon_n - \xi_2), \quad (31)$$

which becomes small as $\varepsilon_n, \xi_1, \xi_2 \rightarrow 0$.

1. Incommensurate combinatorics

In the case of incommensurate (CDW) pseudogap fluctuations, an exact solution for the Green's function of the FGM in the limit as $\xi \rightarrow \infty$ takes a form similar

to (20) [1, 2] and we obtain (averaging (30) with the Rayleigh distribution for W)

$$\begin{aligned} Z(z) &= \int_0^\infty dW \frac{2W}{\Delta^2} e^{-W^2/\Delta^2} \frac{z}{z - W^2} = \\ &= \int_0^\infty \frac{d\zeta}{\Delta^2} e^{-\zeta/\Delta^2} \frac{z}{z - \zeta} = \frac{z}{\Delta^2} e^{-z/\Delta^2} \text{Ei} \left(\frac{z}{\Delta^2} \right). \end{aligned} \quad (32)$$

Then, as $z \rightarrow 0$ we obtain

$$Z(z \rightarrow 0) \approx \frac{z}{\Delta^2} \left[\ln \left(\gamma' \frac{z}{\Delta^2} \right) - i\pi \right]. \quad (33)$$

At the “bare” Fermi surface, we have $\xi_1 = 0$, and we limit ourselves to $\varepsilon_n > 0$ in what follows. From (33), we can then easily find the limit behavior of $Z(z)$. Some of the results are as follows.

1. For $\varepsilon_n \ll |\xi_2|$, we have

$$\text{Re } Z(\varepsilon_n \ll |\xi_2|, \xi_1 = 0) \approx \frac{\pi}{2} \frac{\varepsilon_n |\xi_2|}{\Delta^2}, \quad (34)$$

i.e., the “impure”-like linear behavior in ε_n .

2. For $\varepsilon_n \gg |\xi_2|$ (i.e., also at the “hot spot”, where $\xi_2 = 0$), we have

$$\begin{aligned} \text{Re } Z(\varepsilon_n \gg |\xi_2|, \xi_1 = 0) &\approx \\ &\approx -\frac{\varepsilon_n^2}{\Delta^2} \ln \left(\gamma' \frac{\varepsilon_n^2}{\Delta^2} \right) + \frac{1}{2} \frac{\xi_2^2}{\Delta^2}, \end{aligned} \quad (35)$$

i.e., for $\xi_2 = 0$, the NFL behavior similar to the one-dimensional case.

We note that we always have $\text{Im } Z = 0$ at $\xi_2 = 0$, i.e., at the “shadow” Fermi surface and in particular at the “hot spot” itself.

2. Spin-fermion combinatorics

We now consider the spin-fermion (Heisenberg) model for pseudogap (SDW) fluctuations [2]. In this case, we again obtain the FGM, but with the gap distribution different from the Rayleigh distribution; instead of (32), we have

$$\begin{aligned} Z(z) &= \frac{2}{\sqrt{2\pi}} \int_0^\infty dW \frac{W^2}{\left(\frac{\Delta^2}{3} \right)^{3/2}} \times \\ &\times \exp \left(-\frac{W^2}{2 \left(\frac{\Delta^2}{3} \right)} \right) \frac{z}{z - W^2} = \end{aligned}$$

$$\begin{aligned}
 &= \frac{1}{\sqrt{2\pi}} \int_0^\infty d\zeta \frac{\sqrt{\zeta}}{\left(\frac{\Delta^2}{3}\right)^{3/2}} \exp\left(-\frac{\zeta}{2\left(\frac{\Delta^2}{3}\right)}\right) \frac{\zeta}{z-\zeta} = \\
 &= \frac{\Gamma(3/2)}{\sqrt{2\pi}} \frac{(-z)^{3/2}}{\left(\frac{\Delta^2}{3}\right)^{3/2}} \exp\left[-\frac{z}{2\left(\frac{\Delta^2}{3}\right)}\right] \times \\
 &\quad \times \Gamma\left(-\frac{1}{2}; -\frac{z}{2\left(\frac{\Delta^2}{3}\right)}\right). \quad (36)
 \end{aligned}$$

Hence, as $z \rightarrow 0$, we obtain

$$\begin{aligned}
 Z(z) &\approx \frac{2\Gamma(3/2)}{\sqrt{\pi}} \times \\
 &\times \left[-\frac{z}{2\left(\frac{\Delta^2}{3}\right)} + \Gamma\left(-\frac{1}{2}\right) \left(-\frac{z}{2\left(\frac{\Delta^2}{3}\right)}\right)^{3/2} \right]. \quad (37)
 \end{aligned}$$

On the “bare” Fermi surface ($\xi_p = 0$), we then have

$$\begin{aligned}
 Z(\varepsilon_n \rightarrow 0, \xi_2, \xi_1 = 0) &= \frac{2\Gamma(3/2)}{\sqrt{\pi}} \left[-\frac{\varepsilon_n(\varepsilon_n + i\xi_2)}{2\left(\frac{\Delta^2}{3}\right)} + \right. \\
 &\quad \left. + \Gamma\left(-\frac{1}{2}\right) \left(-\frac{\varepsilon_n(\varepsilon_n + i\xi_2)}{2\left(\frac{\Delta^2}{3}\right)}\right)^{3/2} \right]. \quad (38)
 \end{aligned}$$

In particular, for $\xi_2 = 0$, we have $\text{Im } Z = 0$ and

$$\begin{aligned}
 Z(\varepsilon_n \rightarrow 0, \xi_2 = \xi_1 = 0) &= \\
 = \text{Re } Z(\varepsilon_n \rightarrow 0, \xi_2 = \xi_1 = 0) &= \frac{\Gamma(3/2)}{\sqrt{\pi}} \frac{\varepsilon_n^2}{\left(\frac{\Delta^2}{3}\right)}, \quad (39)
 \end{aligned}$$

and we thus obtain the quadratic NFL behavior of the Z factor. We again present some results on the limit behavior.

1. For $\varepsilon_n \ll |\xi_2|$, we have

$$\begin{aligned}
 \text{Re } Z(\varepsilon_n \ll |\xi_2|, \xi_1 = 0) &= \frac{2\Gamma(3/2)}{\sqrt{\pi}} \times \\
 &\times \left[\frac{\varepsilon_n^2}{2\left(\frac{\Delta^2}{3}\right)} + \sqrt{2\pi} \left(\frac{\varepsilon_n |\xi_2|}{2\left(\frac{\Delta^2}{3}\right)}\right)^{3/2} \right], \quad (40)
 \end{aligned}$$

i.e., the NFL “zero” behavior.

2. For $\varepsilon_n \gg |\xi_2|$ (i.e., also at the “hot spot”, where $\xi_2 = 0$), we have

$$\text{Re } Z(\varepsilon_n \gg \xi_2, \xi_1 = 0) = \frac{\Gamma(3/2)}{\sqrt{\pi}} \frac{\varepsilon_n^2}{\left(\frac{\Delta^2}{3}\right)}, \quad (41)$$

which is again the NFL “zero” behavior.

In the general case of finite correlation lengths $\xi = \kappa^{-1}$, we have to perform numerical analysis using the recursive relations proposed in Refs. [2, 3]. We again use the basic definition of the Z factor in (3). To calculate the self-energy $\Sigma(\varepsilon_n, \xi_p)$ of an electron moving in the quenched random field of (static) Gaussian spin fluctuations with dominant scattering momentum transfers from the vicinity of the characteristic vector \mathbf{Q} , we use the recursive procedure [2, 3] in which all Feynman diagrams describing the scattering of electrons by this random field are taken into account. The sought self-energy is given by

$$\Sigma(\varepsilon_n, \xi_p) = \Sigma_{k=1}(\varepsilon_n, \xi_p) \quad (42)$$

with $\xi_p = \epsilon(\mathbf{p}) - \mu$ (cf. (28)) and

$$\begin{aligned}
 \Sigma_k(\varepsilon_n, \xi_p) &= \\
 &= \Delta^2 \frac{s(k)}{i\varepsilon_n + \mu - \epsilon_k(\mathbf{p}) + inv_k \kappa - \Sigma_{k+1}(\varepsilon_n, \xi_p)}. \quad (43)
 \end{aligned}$$

The quantity Δ again characterizes the energy scale of pseudogap fluctuations and $\kappa = \xi^{-1}$ is the inverse correlation length of short-range SDW fluctuations, $\epsilon_k(\mathbf{p}) = \epsilon(\mathbf{p} + \mathbf{Q})$ and $v_k = |v_{\mathbf{p}+\mathbf{Q}}^x| + |v_{\mathbf{p}+\mathbf{Q}}^y|$ for odd k , while $\epsilon_k(\mathbf{p}) = \epsilon(\mathbf{p})$ and $v_k = |v_{\mathbf{p}}^x| + |v_{\mathbf{p}}^y|$ for even k . The velocity projections $v_{\mathbf{p}}^x$ and $v_{\mathbf{p}}^y$ are determined by the usual momentum derivatives of the “bare” electron energy dispersion $\epsilon(\mathbf{p})$ given by (28). Finally, $s(k)$ is a combinatorial factor, with

$$s(k) = k \quad (44)$$

for commensurate charge (CDW type) fluctuations with $\mathbf{Q} = (\pi/a, \pi/a)$ [5]. For incommensurate CDW fluctuations [5], we find

$$s(k) = \begin{cases} \frac{k+1}{2} & \text{for odd } k, \\ \frac{k}{2} & \text{for even } k. \end{cases} \quad (45)$$

For the spin-fermion model in Ref. [2], the combinatorics of diagrams becomes more complicated. Spin-conserving scattering processes obey commensurate combinatorics, while spin-flip scattering is described by diagrams of the incommensurate type

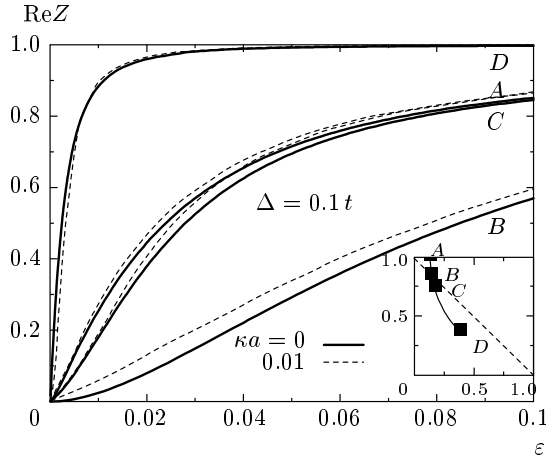


Fig. 4. Dependence of $\text{Re} Z$ on ε_n (in units of t) at different points of the Fermi surface (corresponding to $t' = -0.4t$ and $\mu = -1.3t$) in the “hot spot” model (the spin-fermion combinatorics of diagrams) with the correlation lengths $\xi \rightarrow \infty$ ($\kappa = 0$) and $\xi^{-1}a = \kappa a = 0.01$. The pseudogap amplitude is $\Delta = 0.1t$. Inset: the “bare” Fermi surface and the points where the calculations were done

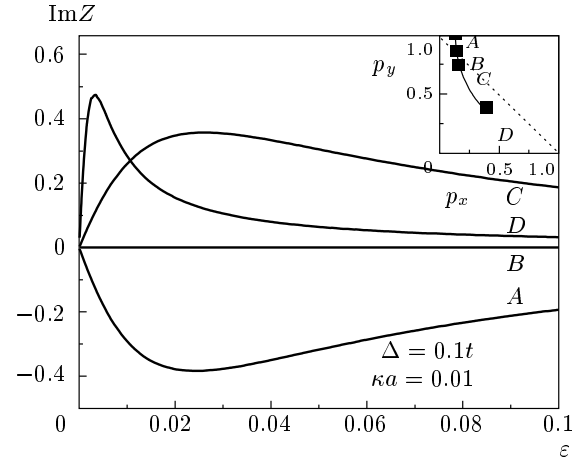


Fig. 5. Dependence of $\text{Im} Z$ on ε_n (in units of the transfer integral t) at different points of the Fermi surface (corresponding to $t' = -0.4t$ and $\mu = -1.3t$) in the “hot spot” model with the finite correlation length $\xi^{-1}a = \kappa a = 0.01$ (the spin-fermion combinatorics of diagrams). The pseudogap amplitude is $\Delta = 0.1t$. Inset: the “bare” Fermi surface and the points where the calculations were done

(“charged” random field in terms of Ref. [2]). In this model, the recursive relation for the single-particle Green’s function is again given by (43), but the combinatorial factor $s(n)$ acquires the form [2]

$$s(k) = \begin{cases} \frac{k+2}{3} & \text{for odd } k, \\ \frac{k}{3} & \text{for even } k. \end{cases} \quad (46)$$

Below, we only present our results for the spin-fermion combinatorics, because in other cases, we obtain more or less similar behavior of the renormalization factors.

In Fig. 4, we show the results of numerical calculation of $\text{Re} Z(\varepsilon_n, \xi_{\mathbf{p}} = 0)$ at different points taken at the “bare” Fermi surface, shown in the inset. For comparison, we show the data obtained in the limit of the infinite correlation length $\xi \rightarrow \infty$ (or $\kappa = 0$, which is an exactly solvable case) and for finite $\kappa a = 0.01$ (i.e., $\xi = 100a$). It is clearly seen that in both cases, $\text{Re} Z \sim 1$ at the “nodal” point D , except at very small values of ε_n , while in the vicinity of the “hot spot” (points A and C) and also at the “hot spot” itself (point B), $\text{Re} Z$ becomes small in a rather wide interval of $\varepsilon_n < \Delta$. This corresponds to an approximately “Fermi-liquid” behavior of the “nodal” region (the vicinity of the Brillouin zone diagonal), with a kind of “marginal” Fermi-liquid or Luttinger-liquid (NFL) behavior as we move to the vicinity of the “hot spot”.

For completeness, in Fig. 5, we show similar comparison of the dependences of $\text{Im} Z$ on ε_n at the same characteristic points on the Fermi surface and for the same parameters as in Fig. 4. It is only important to stress once again that we have $\text{Im} Z = 0$ only at the “hot spot” itself (point B), and therefore Z becomes real and shows the dependence on ε_n more or less equivalent to that proposed for “marginal” Fermi liquids (or Luttinger liquids).

In all cases, we observe the vanishing of the renormalization factor $Z(\varepsilon_n, \xi_{\mathbf{p}})$ at the “bare” Fermi surface. In the absence of static impurity-like scattering due to finite values of the correlation length $\xi = \kappa^{-1}$, the pole singularity of the Green’s function is replaced by a zero, reflecting the topological stability of the “bare” Fermi surface (the Luttinger theorem) [9]. In the presence of this scattering, the singularity of the Green’s function at the topologically stable “bare” Fermi surface remains in the form of a finite discontinuity.

C. Spectral density and Fermi surface “destruction” in the “hot spot” model

We return to (29) and perform the usual analytic continuation to real frequencies, $i\varepsilon_n \rightarrow \varepsilon + i\delta$. We then obtain

$$G^R(\varepsilon, \xi_{\mathbf{p}}) = \frac{\varepsilon - \xi_2}{(\varepsilon + i\delta - \xi_1)(\varepsilon - \xi_2 + i\delta) - W^2} = \frac{\varepsilon - \xi_2}{(\varepsilon - \xi_1)(\varepsilon - \xi_2) - W^2 + i\delta(2\varepsilon - \xi_1 - \xi_2)} \quad (47)$$

and therefore the spectral density in the case of a long-range (CDW, SDW) order is given by

$$A_W(\varepsilon, \xi_{\mathbf{p}}) = -\frac{1}{\pi} \text{Im} G^R(\varepsilon, \xi_{\mathbf{p}}) = (\varepsilon - \xi_2) \delta[(\varepsilon - \xi_1)(\varepsilon - \xi_2) - W^2] \text{sign}(2\varepsilon - \xi_1 - \xi_2). \quad (48)$$

Accordingly, for the FGM with the correlation length $\xi \rightarrow \infty$, we have

$$A(\varepsilon, \xi_{\mathbf{p}}) = \int_0^\infty dW \mathcal{P}_W A_W(\varepsilon, \xi_{\mathbf{p}}), \quad (49)$$

where \mathcal{P}_W is the distribution function of gap fluctuations, depending on the combinatorics of diagrams and leading to the following separate cases, already considered (or mentioned) above.

1. Incommensurate combinatorics

In the case of incommensurate CDW-like pseudogap fluctuations, we have

$$\mathcal{P}_W = \frac{2W}{\Delta^2} \exp\left(-\frac{W^2}{\Delta^2}\right), \quad (50)$$

which is the Rayleigh distribution [4, 11]. From (49), we then obtain

$$A(\varepsilon, \xi_{\mathbf{p}}) = \frac{\varepsilon - \xi_2}{\Delta^2} \exp\left(-\frac{(\varepsilon - \xi_1)(\varepsilon - \xi_2)}{\Delta^2}\right) \times \theta[(\varepsilon - \xi_1)(\varepsilon - \xi_2)] \text{sign}(2\varepsilon - \xi_1 - \xi_2). \quad (51)$$

For $\varepsilon = 0$, we have

$$A(\varepsilon = 0, \xi_{\mathbf{p}}) = \frac{\xi_2}{\Delta^2} \exp\left(-\frac{\xi_1 \xi_2}{\Delta^2}\right) \theta[\xi_1 \xi_2] \text{sign}(\xi_1 + \xi_2). \quad (52)$$

For $\xi_1 \rightarrow \pm 0$, we obtain

$$A(\varepsilon = 0, \xi_{\mathbf{p}} \rightarrow \pm 0, \xi_2) = \pm \frac{\xi_2}{\Delta^2} \theta(\pm \xi_2), \quad (53)$$

and therefore $A(\varepsilon = 0, \xi_{\mathbf{p}})$ is nonzero within the Brillouin zone only in the space between the “bare” Fermi surface and the “shadow” Fermi surface. This qualitative result is confirmed below, for all other combinatorics, in the case of the “pure” FGM with $\xi^{-1} = \kappa = 0$.

2. Commensurate combinatorics

In the case of commensurate CDW-like pseudogap fluctuations, we have [6]

$$\mathcal{P}_W = \frac{1}{\sqrt{2\pi}\Delta} \exp\left(-\frac{W^2}{2\Delta^2}\right), \quad (54)$$

which is the Gaussian distribution. From (49), we then obtain

$$A(\varepsilon, \xi_{\mathbf{p}}) = \frac{1}{\sqrt{2\pi}} \frac{\varepsilon - \xi_2}{\Delta \sqrt{(\varepsilon - \xi_1)(\varepsilon - \xi_2)}} \times \exp\left(-\frac{(\varepsilon - \xi_1)(\varepsilon - \xi_2)}{2\Delta^2}\right) \times \theta[(\varepsilon - \xi_1)(\varepsilon - \xi_2)] \text{sign}(2\varepsilon - \xi_1 - \xi_2), \quad (55)$$

with the same qualitative conclusions as in the incommensurate case.

3. Spin-fermion combinatorics

In the case of SDW-like pseudogap fluctuations of the (Heisenberg) spin-fermion model [2], we have the gap distribution

$$\mathcal{P}_W = \frac{2}{\pi} \frac{W^2}{\left(\frac{\Delta^2}{3}\right)^{3/2}} \exp\left(-\frac{W^2}{2\left(\frac{\Delta^2}{3}\right)}\right). \quad (56)$$

From (49), we then obtain

$$A(\varepsilon, \xi_{\mathbf{p}}) = \frac{1}{\sqrt{2\pi}} \frac{\sqrt{(\varepsilon - \xi_1)(\varepsilon - \xi_2)}}{\left(\frac{\Delta^2}{3}\right)^{3/2}} \times \exp\left(-\frac{(\varepsilon - \xi_1)(\varepsilon - \xi_2)}{2\left(\frac{\Delta^2}{3}\right)}\right) \theta[(\varepsilon - \xi_1)(\varepsilon - \xi_2)] \times \text{sign}(2\varepsilon - \xi_1 - \xi_2), \quad (57)$$

again with the same qualitative conclusions as in the incommensurate case.

In the general case of finite correlation lengths $\xi = \kappa^{-1}$, spectral densities can be directly computed using analytic continuation of recursive relations (42) and (43) to real frequencies [2, 3].

Actually, two-dimensional contour plots of $A(\varepsilon = 0, \xi_{\mathbf{p}})$ (which directly correspond to ARPES intensity plots) can be used for a “practical” definition of the renormalized Fermi surface and provide a

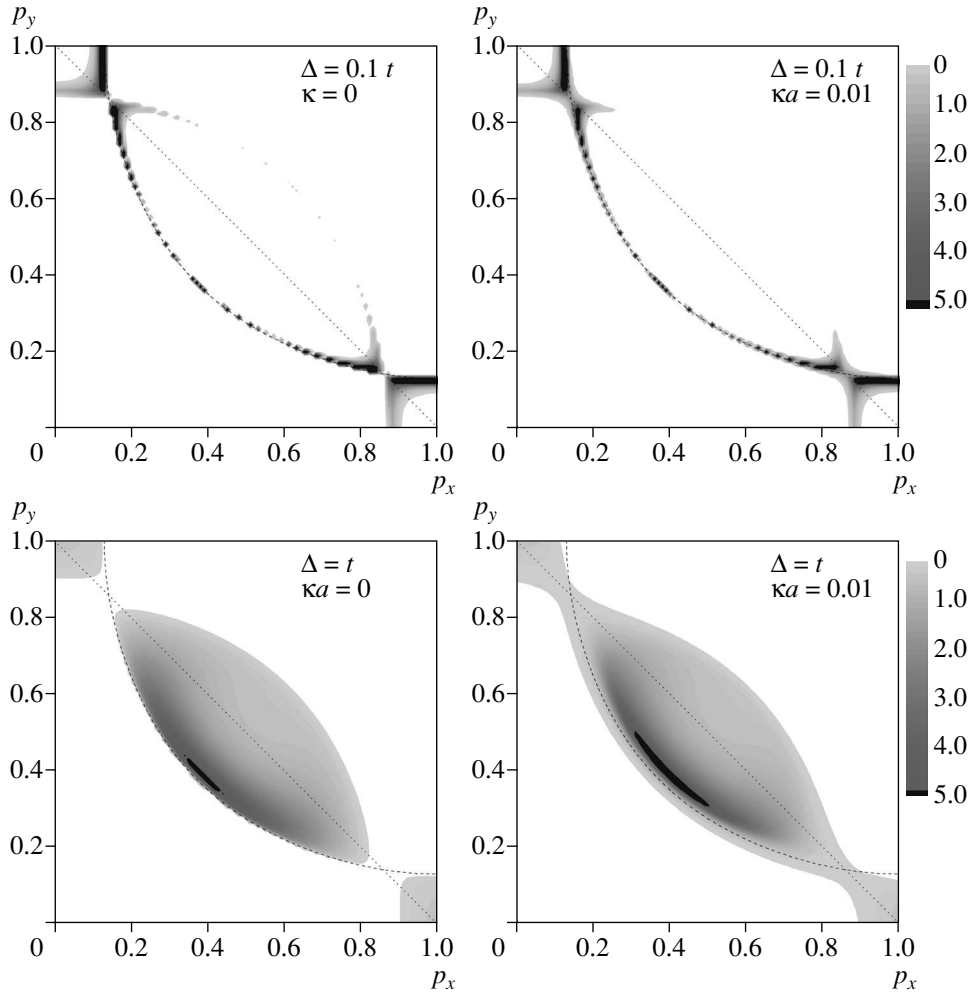


Fig. 6. Intensity plots of the spectral density $A(\varepsilon = 0, \xi_{\mathbf{p}})$ in the Brillouin zone for the “hot spots” model ($t' = -0.4t$ and $\mu = -1.3t$) in the case of infinite correlation length $\xi^{-1} = \kappa = 0$ and for a finite correlation length $\xi^{-1}a = \kappa a = 0.01$ (the spin-fermion combinatorics of diagrams) with different values of the pseudogap amplitude. The “bare” Fermi surface is shown by a dashed line

qualitative picture of its evolution in the FGM with changed model parameters⁶⁾.

In Fig. 6, we show typical intensity plots of the spectral density $A(\varepsilon = 0, \xi_{\mathbf{p}})$ in the Brillouin zone for the “hot spot” model both in the case of the infinite correlation length $\xi^{-1} = \kappa = 0$ and for a finite (large!) correlation length $\xi^{-1}a = \kappa a = 0.01$ (for the spin-fermion combinatorics of diagrams; in other cases, the behavior is quite similar) and for different values of the pseudogap amplitude Δ . We see that these spectral density plots give a rather beautiful qualitative picture of the

“destruction” of the Fermi surface in the vicinity of “hot spots” for small values of Δ , with formation of typical “Fermi arcs” as Δ grows, which qualitatively resembles typical ARPES data for copper oxides [16, 17].

D. Superconducting d -wave fluctuations

As noted above, the case of superconducting s -wave pseudogap fluctuations simply reduces to the one-dimensional FGM. Much more interesting is the case of superconducting d -wave fluctuations in two dimensions.

To obtain exact results in the case of the infinite correlation length $\xi^{-1} = \kappa = 0$, we have only to make simple replacements in the above expressions for the

⁶⁾ We note that for free electrons, $A(\varepsilon = 0, \xi_{\mathbf{p}}) = \delta(\xi_{\mathbf{p}})$, and therefore the appropriate intensity plot directly reproduces the “bare” Fermi surface.

“hot spot” model with incommensurate combinatorics: $\xi_2 \rightarrow -\xi_1 = -\xi_{\mathbf{p}}$ and $\Delta \rightarrow \Delta_{\mathbf{p}}$, where $\Delta_{\mathbf{p}}$ defines the amplitude of fluctuations with the d -wave symmetry:

$$\Delta_{\mathbf{p}} = \frac{1}{2}\Delta [\cos(p_x a) - \cos(p_y a)], \quad (58)$$

where Δ now characterizes the energy scale of pseudogap fluctuations.

Equation (31) then reduces to $z = -(\varepsilon_n^2 + \xi_{\mathbf{p}}^2)$ and we immediately obtain an expression for the Z factor, similar to (21):

$$\begin{aligned} Z(\varepsilon_n, \xi_{\mathbf{p}}) &= -\frac{\varepsilon_n^2 + \xi_{\mathbf{p}}^2}{\Delta_{\mathbf{p}}^2} \exp\left(-\frac{\varepsilon_n^2 + \xi_{\mathbf{p}}^2}{\Delta_{\mathbf{p}}^2}\right) \times \\ &\times \text{Ei}\left(-\frac{\varepsilon_n^2 + \xi_{\mathbf{p}}^2}{\Delta_{\mathbf{p}}^2}\right) \approx -\frac{\varepsilon_n^2 + \xi_{\mathbf{p}}^2}{\Delta_{\mathbf{p}}^2} \times \\ &\times \ln\left(\gamma \frac{\varepsilon_n^2 + \xi_{\mathbf{p}}^2}{\Delta_{\mathbf{p}}^2}\right) \rightarrow 0 \quad \text{as } \varepsilon_n \rightarrow 0, \quad \xi_{\mathbf{p}} \rightarrow 0, \quad (59) \end{aligned}$$

again replacing the pole singularity by a zero at the “bare” Fermi surface, except for the “nodal” point at the diagonal of the Brillouin zone, where $\Delta_{\mathbf{p}} = 0$ (cf. (58)).

Instead of (51), we obtain the spectral density as

$$\begin{aligned} A(\varepsilon, \xi_{\mathbf{p}}) &= \frac{\varepsilon + \xi_{\mathbf{p}}}{\Delta_{\mathbf{p}}^2} \exp\left(-\frac{\varepsilon^2 - \xi_{\mathbf{p}}^2}{\Delta_{\mathbf{p}}^2}\right) \times \\ &\times \theta(\varepsilon^2 - \xi_{\mathbf{p}}^2) \text{sign } \varepsilon, \quad (60) \end{aligned}$$

which is nonzero only for $|\xi_{\mathbf{p}}| < \varepsilon$. As a result, at $\varepsilon = 0$, we have $A(\varepsilon = 0, \xi_{\mathbf{p}}) = 0$ for $\Delta_{\mathbf{p}} \neq 0$, and it is different from zero only at the intersection of the Brillouin zone diagonal with the “bare” Fermi surface, where $\Delta_{\mathbf{p}}$ given by (58) is zero. At the Fermi surface itself, we have

$$A(\varepsilon, \xi_{\mathbf{p}} = 0) = \frac{|\varepsilon|}{\Delta_{\mathbf{p}}^2} \exp\left(-\frac{\varepsilon^2}{\Delta_{\mathbf{p}}^2}\right), \quad (61)$$

with two maxima at $\varepsilon = \pm \Delta_{\mathbf{p}}/\sqrt{2}$.

Considering the general case of finite correlation lengths $\xi = \kappa^{-1}$, we again perform numerical analysis based on the recursive relations introduced for this problem in Ref. [3], using the basic definition of the Z factor in (3). To calculate the self-energy $\Sigma(\varepsilon_n, \xi_{\mathbf{p}})$ of an electron scattered by static fluctuations of the superconducting order parameter with the d -wave symmetry, we use the following relation (similar to (43)) slightly generalizing relations derived in Ref. [3]:

$$\begin{aligned} \Sigma_k(\varepsilon_n, \xi_{\mathbf{p}}) &= \\ &= \frac{\Delta_{\mathbf{p}}^2 s(k)}{i\varepsilon_n - (-1)^k \xi_{\mathbf{p}} + ik\kappa(|v_{\mathbf{p}}^x| + |v_{\mathbf{p}}^y|) - \Sigma_{k+1}(\varepsilon_n, \xi_{\mathbf{p}})}, \quad (62) \end{aligned}$$

where $s(k)$ is defined in (45).

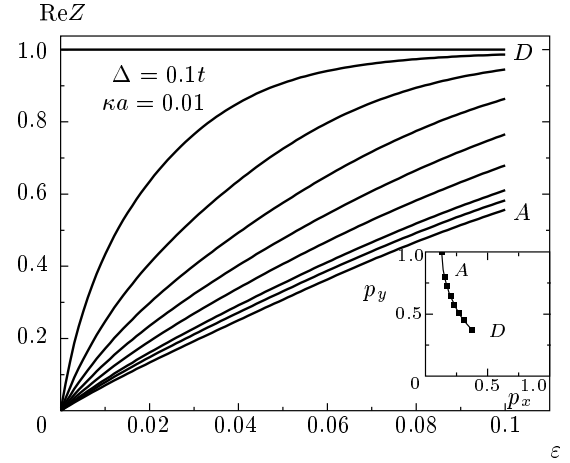


Fig. 7. The dependences of $\text{Re } Z$ on ε_n (in units of t) at different points of the Fermi surface (corresponding to $t' = -0.4t$ and $\mu = -1.3t$) in the model of superconducting (d -wave) pseudogap fluctuations with the correlation length $\xi^{-1}a = \kappa a = 0.01$. The pseudogap amplitude is $\Delta = 0.1t$. Inset: the “bare” Fermi surface and the points where the calculations were done

In Fig. 7, we show the results for $\text{Re } Z(\varepsilon_n, \xi_{\mathbf{p}} = 0)$, again taken at different points of the “bare” Fermi surface, shown in the inset. The correlation length is $\xi = 100a$ ($\kappa a = 0.01$) and $\Delta = 0.1t$. It is clearly seen that $\text{Re } Z = 1$ precisely at the “nodal” point D (where $\Delta_{\mathbf{p}} = 0$), but at other points on the “bare” Fermi surface, $\text{Re } Z$ is strongly renormalized in a rather wide intervals of $\varepsilon_n < |\Delta_{\mathbf{p}}|$, tending to zero as $\varepsilon_n \rightarrow 0$. We thus again obtain a kind of “marginal” Fermi liquid or Luttinger liquid (NFL), but qualitatively different from the case of “hot spot” model.

In Fig. 8, we also show typical intensity plots of the spectral density $A(\varepsilon = 0, \xi_{\mathbf{p}})$ in the Brillouin zone in the case of superconducting (d -wave) pseudogap fluctuations with the correlation length $\xi^{-1}a = \kappa a = 0.1$ and two different values of Δ . We see that these spectral density plots give a totally different picture of the “destruction” of the Fermi surface than the one given by the “hot spot” model, which also, in our opinion, differs significantly from most results of the ARPES measurements on copper oxides. The Fermi surface is sharply defined only at one point (at the diagonal of the Brillouin zone), where $\Delta_{\mathbf{p}}$ given by (58) is precisely zero, and there are no sharply defined Fermi arcs formed close to this point. We observe only some more or less wide “dragonfly wings” formed around this point. We also note the absence of any signs of the “shadow” Fermi surface.

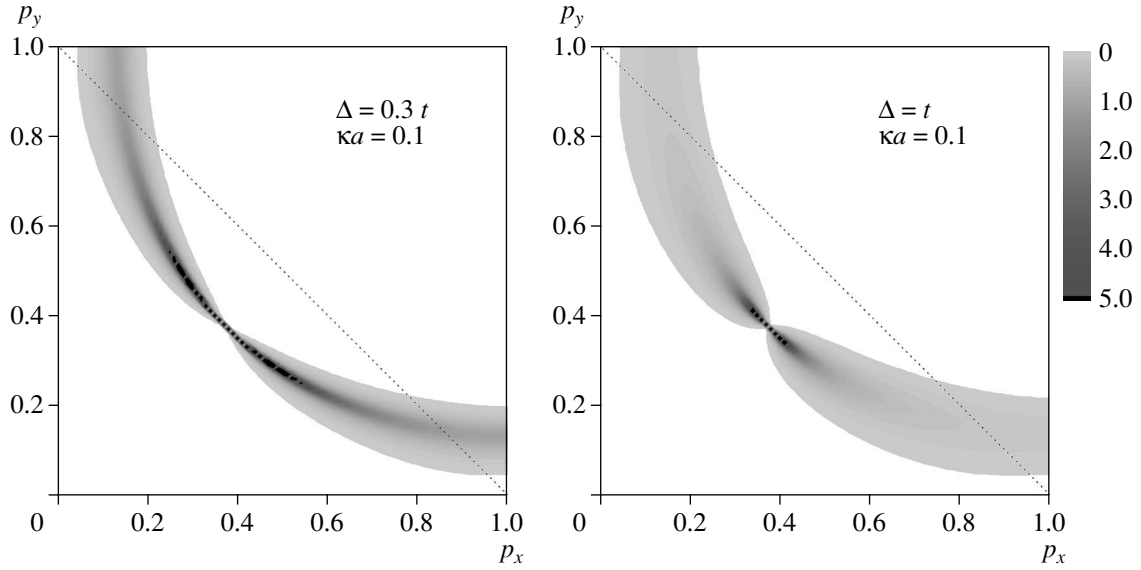


Fig. 8. Intensity plots of the spectral density $A(\varepsilon = 0, \xi_p)$ in the Brillouin zone ($t' = -0.4t$ and $\mu = -1.3t$) in the case of superconducting (d -wave) pseudogap fluctuations. The correlation length is $\xi^{-1}a = \kappa a = 0.1$ (with the spin-fermion combinatorics of diagrams) for two different values of the pseudogap amplitude $\Delta = 0.3t$ and $\Delta = t$

4. CONCLUSION

We analyzed the rather unusual (NFL) behavior of the fluctuating gap model of pseudogap behavior in both one and two dimensions. We studied the quasiparticle renormalization (Z factor) of the single-electron Green's function, demonstrating a kind of "marginal" Fermi-liquid or Luttinger-liquid behavior (i.e., the absence of well-defined quasiparticles close to the Fermi surface) and also the topological stability of the "bare" Fermi surface (the Luttinger theorem). This reflects strong renormalization effects leading to the replacement of the usual pole singularity of the Green's function in a Fermi liquid by a zero, thus effectively replacing the Fermi surface of poles by the Luttinger surface of zeroes [20]. In the presence of static impurity-like scattering due to the effects of finite correlation lengths of pseudogap fluctuations, this singularity is replaced by a finite discontinuity.

In the two-dimensional case, we discussed the effective picture of the Fermi surface "destruction" both in the "hot spot" model of dielectric (AFM, CDW) pseudogap fluctuations and in the qualitatively different case of superconducting d -wave fluctuations, reflecting the NFL spectral density behavior and similar to that observed in ARPES experiments on copper oxides. Intensity plots obtained in the case of AFM (CDW) fluctuations, in our opinion, are more similar to the ARPES intensity data obtained in experiments

on copper oxides. We note that this effective picture was also directly generalized to the case of strongly correlated metals or doped Mott insulators [18] using the so-called $DMFT + \Sigma_k$ approach in Ref. [19].

The authors are grateful to G. E. Volovik for his interest and very useful discussions, which, in fact, initiated this work.

This work was supported in part by the RFBR (grant № 05-02-16301) and programs of the Presidium of the Russian Academy of Sciences (RAS) "Quantum macrophysics" and of the Division of Physical Sciences of the RAS "Strongly correlated electrons in semiconductors, metals, superconductors, and magnetic materials".

REFERENCES

1. M. V. Sadovskii, Usp. Fiz. Nauk **171**, 539 (2001); E-print archives, cond-mat/0408489.
2. J. Schmalian, D. Pines, and B. Stojkovic, Phys. Rev. B **60**, 667 (1999).
3. E. Z. Kuchinskii and M. V. Sadovskii, Zh. Eksp. Teor. Fiz. **115**, 1765 (1999).
4. M. V. Sadovskii, Zh. Eksp. Teor. Fiz. **66**, 1720 (1974); Fiz. Tverd. Tela **16**, 2504 (1974).

5. M. V. Sadovskii, Zh. Eksp. Teor. Fiz. **77**, 2070 (1979).
6. W. Wonneberger and R. Lautenschlager, J. Phys. C **9**, 2865 (1976).
7. M. V. Sadovskii and A. A. Timofeev, J. Moscow. Phys. Soc. **1**, 391 (1991).
8. R. H. McKenzie and D. Scarratt, Phys. Rev. **54**, R12709 (1996).
9. G. E. Volovik, E-print archives, cond-mat/0505089; cond-mat/0601372.
10. A. B. Migdal, *Theory of Finite Fermi Systems and Applications to Atomic Nuclei*, Interscience Publishers, New York (1967); Nauka, Moscow (1983).
11. M. V. Sadovskii, *Diagrammatics*, World Scientific, Singapore (2006).
12. I. E. Dzyaloshinskii and A. I. Larkin, Zh. Eksp. Teor. Fiz. **65**, 411 (1973).
13. C. M. Varma, P. B. Littlewood, S. Schmitt-Rink, E. Abrahams, and A. E. Ruckenstein, Phys. Rev. Lett. **63**, 1996 (1989).
14. M. V. Sadovskii and N. A. Strigina, Zh. Eksp. Teor. Fiz. **122**, 610 (2002).
15. M. V. Sadovskii, Physica C **341-348**, 811 (2000).
16. M. R. Norman, H. Ding, M. Randeria, J. C. Campuzano, T. Yokoya, T. Takeuchi, T. Takahashi, T. Mochiku, K. Kadowaki, P. Guptasarma, and D. G. Hinks, Nature **392**, 157 (1998).
17. A. A. Kordyuk, S. V. Borisenko, M. S. Golden, S. Legner, K. A. Nenkov, M. Knupfer, J. Fink, H. Berger, L. Forro, and R. Follath, Phys. Rev. B **66**, 014502 (2002).
18. E. Z. Kuchinskii, I. A. Nekrasov, and M. V. Sadovskii, Pis'ma v Zh. Eksp. Teor. Fiz. **82**, 217 (2005).
19. M. V. Sadovskii, I. A. Nekrasov, E. Z. Kuchinskii, Th. Pruschke, and V. I. Anisimov, Phys. Rev. B **72**, 155105 (2005).
20. I. E. Dzyaloshinskii, Phys. Rev. B **68**, 085113 (2003).